Am J Cancer Res 2016;6(11):2514-2531
www.ajcr.us /ISSN:2156-6976/ajcr0030297

Original Article

Combined VEGFR and CTLA-4 blockade increases the antigen-presenting function of intratumoral DCs and reduces the suppressive capacity of intratumoral MDSCs

Stephanie Du Four[1], Sarah K Maenhout[1], Simone P Niclou[3], Kris Thielemans[1,2], Bart Neyns[2], Joeri L Aerts[1]

[1]Laboratory of Molecular and Cellular Therapy, Vrije Universiteit Brussel, Laarbeeklaan 103E, 1090, Brussels, Belgium; [2]Department of Medical Oncology, UZ Brussel, Laarbeeklaan 101, 1090, Brussels, Belgium; [3]NORLUX Neuro-Oncology Laboratory, Luxembourg Institute of Health (LIH), Luxembourg

Received April 11, 2016; Accepted April 24, 2016; Epub November 1, 2016; Published November 15, 2016

Abstract: Melanoma brain metastases (MBM) occur in 10% to 50% of melanoma patients. They are often associated with a high morbidity and despite the improvements in the treatment of advanced melanoma, including immunotherapy, patients with MBM still have a poor prognosis. Antiangiogenic treatment was shown to reduce the immunosuppressive tumor microenvironment. Therefore we investigated the effect of the combination of VEGFR- and CTLA-4 blockade on the immune cells within the tumor microenvironment. In this study we investigated the effect of the combination of axitinib, a TKI against VEGFR-1, -2 and -3, with therapeutic inhibition of CTLA-4 in subcutaneous and intracranial mouse melanoma models. The combination of axitinib with αCTLA-4 reduced tumor growth and increased survival in both intracranial and subcutaneous models. Investigation of the splenic immune cells showed an increased number of $CD4^+$ and $CD8^+$ T cells after combination treatment. Moreover, combination treatment increased the number of intratumoral dendritic cells (DCs) and monocytic myeloid-derived suppressor cells (moMDSCs). When these immune cell populations were sorted from the subcutaneous and intracranial tumors of mice treated with axitinib+αCTLA-4, we observed an increased antigen-presenting function of DCs and a reduced suppressive capacity of moMDSCs on a per cell basis. Our results suggest that the combination of antiangiogenesis and checkpoint inhibition can lead to an enhanced antitumor effect leading to increased survival. We found that this effect is in part due to an enhanced antitumor immune response generated by an increased antigen-presenting function of intratumoral DCs in combination with a reduced suppressive capacity of intratumoral moMDSCs.

Keywords: MDSC, melanoma brain metastases, antiangiogenesis, CTLA-4 blockade, DCs, tumor microenvironment

Introduction

Patients with advanced melanoma have a high risk of developing brain metastases. The frequency of melanoma brain metastases (MBM) in these patients ranges from 10% to 50% and autopsy series suggest even higher frequencies (66% to 75%) [1].

Over the past few years the overall survival (OS) of advanced melanoma patients has improved with the introduction of BRAF- and MEK-inhibitors (resp. dabrafenib, vemurafenib and trametinib) and immune checkpoint blockers including monoclonal antibodies against Cytotoxic T Lymphocyte Antigen 4 (CTLA-4) and Programmed Death 1 (PD-1) (resp. ipilimumab and nivolumab, pembrolizumab) [2-7]. In patients with MBM, positive for BRAF V600 mutations, treatment with dabrafenib and vemurafenib led to objective response rates (ORR) of respectively 30% and 42% and median OS (mOS) of approximately 8 months and 5.2 months respectively, demonstrating their intracranial activity [8, 9]. Treatment with ipilimumab led to a mOS of 7 months and 3.7 months in respectively asymptomatic MBM patients and symptomatic corticosteroid-dependent MBM patients [10]. Hence, despite these promising results in advanced melanoma, the prognosis of patients with MBM still remains poor.

Over the past few years it has been shown that antiangiogenic treatment has beneficial effects on tumor growth, but also has favorable effects on antitumor immunity. This is due to the fact that elevated levels of circulating Vascular Endothelial Growth Factor (VEGF) exert negative effects on immune cells through several mechanisms, including suppression of dendritic cell (DC) maturation, promotion of regulatory T cell (T_{reg}) proliferation, attraction of myeloid-derived suppressor cells (MDSCs) and induction of a pro-angiogenic and immunosuppressive M2-like phenotype in tumor-associated macrophages (TAMs). In addition, the imbalance of the VEGF-VEGFR-signaling pathway present in the tumor microenvironment results in leaky immature blood vessels and high interstitial pressure limiting influx of immune cells in the tumor [11-14]. However, it has been shown that VEGF-VEGFR-blockade not only induces maturation of immature blood vessels and leads to a reduction in interstitial pressure, but also reduces the number of MDSCs, repolarizes the TAMs to an M1-like phenotype and increases intratumoral T-cell infiltration [11, 15]. Additionally, we have previously shown in subcutaneous and intracranial mouse melanoma models that VEGFR-blockade reduces the suppressive capacity of monocytic MDSCs (moMDSCs) and induces an antigen-presenting capacity in these cells [16].

The effect of CTLA-4 blockade on MDSCs has not been extensively investigated. In melanoma patients a higher number of circulating MDSCs was observed and their number increases with metastatic spread. Treatment with ipilimumab decreased the number of circulating MDSCs, more specifically the granulocytic MDSCs (grMDSCs), and reduced numbers of MDSCs were correlated with improved outcome of melanoma patients. In addition, ipilimumab reduced the arginase-1 production of these grMDSCs, which is their most commonly described suppressive mechanism [17-19].

Therefore we investigated whether the combination of axitinib, a tyrosine kinase inhibitor (TKI) against VEGFR-1, -2 and -3, with a monoclonal antibody blocking CTLA-4 synergistically affects tumor growth and the frequency and function of several immune cell populations, specifically MDSCs, in subcutaneous and intracranial melanoma mouse models.

Material and methods

Tumor cell lines

The mouse melanoma cell line B16F1 was purchased from the American Type Culture Collection (ATCC) and was cultured in Dulbecco's Modified Eagle Medium (DMEM, Sigma) supplemented with 5% fetal clone I (FCI), 100 U/ml penicillin, 100 µg/ml streptomycin, 2 mM L-glutamine, 1 mM sodium pyruvate and non-essential amino acids. To allow *in vivo* bioluminescence imaging of intracranial tumors, B16F1 cells were transduced with a lentiviral construct encoding both tNGFR and FLuc (pHR trip CMV luc2-Ires-tNGFR SIN, described in Goyvaerts *et al.*) [20]. Stable and highly FLuc positive B16F1 cells were subsequently enriched by cell sorting using the expression levels of the tNGFR protein as a reference. We refer to the stable luciferase-expressing cell line used as B16F1-FLuc. The growth rate of B16F1-FLuc cells was similar to that of the parental line. No full authentication of the cell lines was carried out. Cell lines were tested for their known characteristics including expression of antigens and MHC molecules by reverse transcriptase PCR or flow cytometry and their *in vitro* and *in vivo* growth characteristics were closely monitored.

Mice and tumor models

Female and male, 6- to 12-week-old C57BL/6 (CD45.2 congenic) and C3H mice were purchased from Charles River (L'Arbresle Cedex, France). Pmel-1 TCR (T cell receptor transgene specific for the mouse homologue pmel of the human premelanosome protein gp100) transgenic mice. were were kindly provided by Dr. Thorbald van Hall (Leiden University Medical Center) and sequentially bred in house. The Vβ-13-pmel-1 TCR recognizes an epitope of the gp100 melanoma/melanocyte differentiation antigen present on the B16F1 melanoma. All animals were bred, housed and handled according to the European guidelines for animal experimentation. All experiments were reviewed and approved by the ethical committee for use of laboratory animals of the Vrije Universiteit Brussel. For the induction of subcutaneous tumors, mice were anesthetized by inhalation of isoflurane (Abbvie) and inoculated with 5 x 10^5 B16F1 tumor cells in the lower

back. For the induction of intracranial tumors, mice were anesthetized through intraperitoneal injection of ketamine (70 mg/kg; Ceva) and xylazine (10 mg/kg; Bayer) and 1 x 10^4 B16F1 cells or B16F1-FLuc cells were stereotactically implanted into the brain (1 mm anterior to the bregma and 2 mm to the right of the midline suture at a depth of 2.5 mm).

Treatment of tumor-bearing mice with axitinib

Axitinib was kindly provided by Mike Sullivan from Pfizer. For the subcutaneous tumor model, mice were randomly divided into a control group and a treatment group. When tumors reached a volume of approximately 100 mm^3, mice were dosed orally with vehicle or axitinib (25 mg/kg), respectively. Mice were treated by oral gavage, bid, for a period of 7 days. Mice were injected intraperitoneally with 100 µg anti-mouse CTLA-4 (5 mg/kg, clone 9H10) or hamster IgG1 isotype controle (both from BioXCell) on day 2, 4 and 6 of axitinib treatment for *in vivo* assays and on day 2, 4, 6 and 8 for survival experiments.

Tumors were measured every 2 days and tumor volume was calculated using the following formula: V = [(smallest diameter)^2 x largest diameter)]/2. Mice were sacrificed when tumors reached a volume of 2.500 mm^3. For the intracranial tumor model, 7 days after tumor inoculation, mice were randomly divided into a control group and a treatment group and were treated as described above. Tumor growth was measured by means of *in vivo* bioluminescence. Mice were monitored and sacrificed when they displayed established signs of distress or discomfort, including development of cachexia (as defined by a loss of 20% of original body weight), limb paresis, or paralysis and the inability to move and reach for the food source.

Preparation of a single cell suspension from spleen and tumor of tumor-bearing mice

For some experiments, tumor-bearing mice were sacrificed on the last day of treatment with axitinib or vehicle and spleens and tumors were isolated. Single cell spleen suspensions were treated with Tris-buffered ammonium chloride (RBC lysis buffer) for 5 min to remove red blood cells. Tumors were isolated and minced into small pieces followed by a mechanical dissociation step using the GentleMACS dissociator. Samples were then incubated for 40 min at 37°C with the following enzymes: collagenase I (10,000 U/ml; Sigma) and dispase II (32 mg/ml; Roche). After a last mechanical disruption step, the digested tumor tissue was harvested, filtered (over a 70 µM nylon filter, BD Falcon) and red blood cells were lysed by adding RBC lysis buffer.

In vivo bioluminescence assay

In vivo bioluminescence imaging (BLI) was performed on intracranial tumor-bearing mice to follow tumor growth. Mice were imaged every three days. Before and during imaging, mice were anesthetized with isoflurane (2%). Prior to imaging, 50 µL of 30 mg/ml luciferase substrate, D-Luciferin (Promega), in 0.9% NaCl (Braun) was injected intravenously. Mice were shaved over the intracranial injection site of tumor cells to minimize the amount of light absorbed by the black fur. A cooled charge coupled device camera apparatus (PhotonImager, Optima, Biospace lab) was used to detect photon emission from tumor-bearing mice with an acquisition time of 5 min. Analysis was performed as previously described [21].

Phenotypical characterization of immune cells

In order to evaluate the phenotype of different immune cell populations, cells derived from the spleen or tumor of vehicle- or axitinib-treated mice were stained with the following antibodies: phycoerythrin (PE)-Cy7-conjugated anti-mouse CD3 (BioLegend), Alexa Fluor 700 (AF700)-conjugated anti-mouse CD4 (BD Biosciences), AF647-conjugated anti-mouse CD8 (BioLegend), Horizon V450-conjugated anti-mouse CD45 (BD Biosciences), peridinin chlorophyll protein (PerCP)-Cy5.5-conjugated anti-mouse CD4 (BD Biosciences), PE-conjugated anti-mouse CD25 (eBioscience), AF647-conjugated anti-mouse CD11c (BioLegend), PE-conjugated anti-mouse CD11b (BD Biosciences), fluorescein isothiocyanate (FITC)-conjugated anti-mouse CD86 (BD Biosciences), biotin-conjugated anti-mouse CD80 (BD Biosciences) with streptavidin-allophycocyanin (APC)-H7 antibody (BD Biosciences), FITC-conjugated anti-mouse CD11b (BD Biosciences), AF647-conjugated anti-mouse Ly6G (BioLegend) and PECy7-conjugated anti-mouse Ly6C (BioLegend).

Restimulation assay

In order to evaluate if there were antigen-specific T cells present in the spleen of tumor-bearing mice, splenocytes were isolated, labeled with 0.5 μM CellTrace™ Violet (Invitrogen) and seeded in 96-well plates at 2 x 10^5 cells per well in the presence of TRP-2-peptide at a concentration of 5 μM (Sigma-Aldrich). After 3 days, proliferation of $CD4^+$ and $CD8^+$ T cells was analyzed by flow cytometry by staining with PerCPCy5.5-conjugated anti-mouse CD3 (BioLegend), AF700-conjugated anti-mouse CD4 (BD Biosciences) and APCH7-conjugated anti-mouse CD8 (BD Biosciences) antibodies. In addition, supernatants collected 3 days after co-culture were subjected to enzyme-linked immunosorbent assay (ELISA) to quantify cytokine secretion.

Purification of MDSCs from spleen and tumor and DCs from the tumor

To study the function of splenic MDSCs, the $CD11b^+$ fraction was enriched by MACS sorting using $CD11b^+$ Microbeads (Miltenyi Biotec) and to assess the function of tumor-infiltrating MDSCs the $CD45^+$ fraction was enriched by MACS sorting using $CD45^+$ MicroBeads (Miltenyi Biotec). These enriched $CD11b^+$ cells (spleen) or $CD45^+$ cells (tumor) were then stained with Brilliant Violet 605-conjugated anti-CD45 (BD Biosciences) FITC-conjugated anti-CD11b (BD Biosciences), APC-labeled anti-Ly6G (BioLegend) and PE-Cy7-conjugated anti-Ly6C (BioLegend). Subsets of MDSCs were sorted to a purity of > 90% using a BD FACSAria III cell sorter (BD Biosciences). For sorting of intratumoral DCs the enriched $CD45^+$ cells were stained with BV605-conjugated anti-CD45 (BD Biociences) FITC-conjugated anti-CD11b (BD Biosciences) and AF647-conjugated anti-mouse CD11c (BioLegend).

Suppression assay

The suppressive activity of MDSCs was determined using standard proliferation assays as described before [22]. Briefly, splenocytes were isolated from naive mice, labeled with 0.5 μM CellTrace™ Violet (Invitrogen) and seeded in 96-well plates at 2 x 10^5 cells per well. Purified MDSCs were then added at different ratios (MDSC:splenocytes), 1:8 (spleen), 1:10 (subcutaneous tumor) and 1:4 (intracranial tumor). T-cell proliferation was induced by Dynabeads® Mouse T-activator CD3/CD28 beads (Invitrogen). After 3 days, proliferation of $CD4^+$ and $CD8^+$ T cells was analyzed by flow cytometry by staining with PerCPCy5.5-conjugated anti-mouse CD3 (BioLegend), AF700-conjugated anti-mouse CD4 (BD Biosciences) and APCH7-conjugated anti-mouse CD8 (BD Biosciences) antibodies. The percentage of T-cell suppression was calculated using the following formula: % suppression = [1 - (% proliferation with MDSC/ % proliferation without MDSC)] x 100.

In addition, supernatants collected 3 days after co-culture were subjected to ELISA to quantify cytokine secretion.

DC stimulation assay

Spleen-derived pmel $CD8^+$ T cells were enriched by MACS sorting using CD8 MicroBeads (Miltenyi Biotec), were subsequently labeled with 0.5 μM CellTrace™ Violet (Invitrogen) and seeded in 96-well plates. Purified DCs were then added at a 1:10 ratio (DC:splenocytes). After 3 days, proliferation of pmel $CD8^+$ T cells was analyzed by flow cytometry by staining with PerCPCy5.5-conjugated anti-mouse CD3 (BioLegend), AF700-conjugated anti-mouse CD4 (BD Biosciences) and APCH7-conjugated anti-mouse CD8 (BD Biosciences) antibodies. In addition, supernatants collected 3 days after co-culture were subjected to ELISA to quantify cytokine secretion.

Allogeneic mixed lymphocyte reaction

Spleen-derived $CD8^+$ T cells (from C3H mice) were enriched by MACS sorting using CD8 MicroBeads (Miltenyi Biotec), were subsequently labeled with 0.5 μM CellTrace™ Violet (Invitrogen) and seeded in 96-well plates at 2 x 10^5 cells per well. Purified allogeneic monocytic MDSCs (sorted from tumors of C57BL/6 mice) were then added at different ratios 1:10, 1:20 and 1:40 (MDSC:splenocytes). After 3 days, proliferation of $CD8^+$ T cells was analyzed by flow cytometry by staining with PerCPCy5.5-conjugated anti-mouse CD3 (BioLegend), AF-700-conjugated anti-mouse CD4 (BD Biosciences) and APC-H7-conjugated anti-mouse CD8 (BD Biosciences) antibodies. In addition, supernatants were collected 3 days after co-culture for determination of cytokine secretion by ELISA.

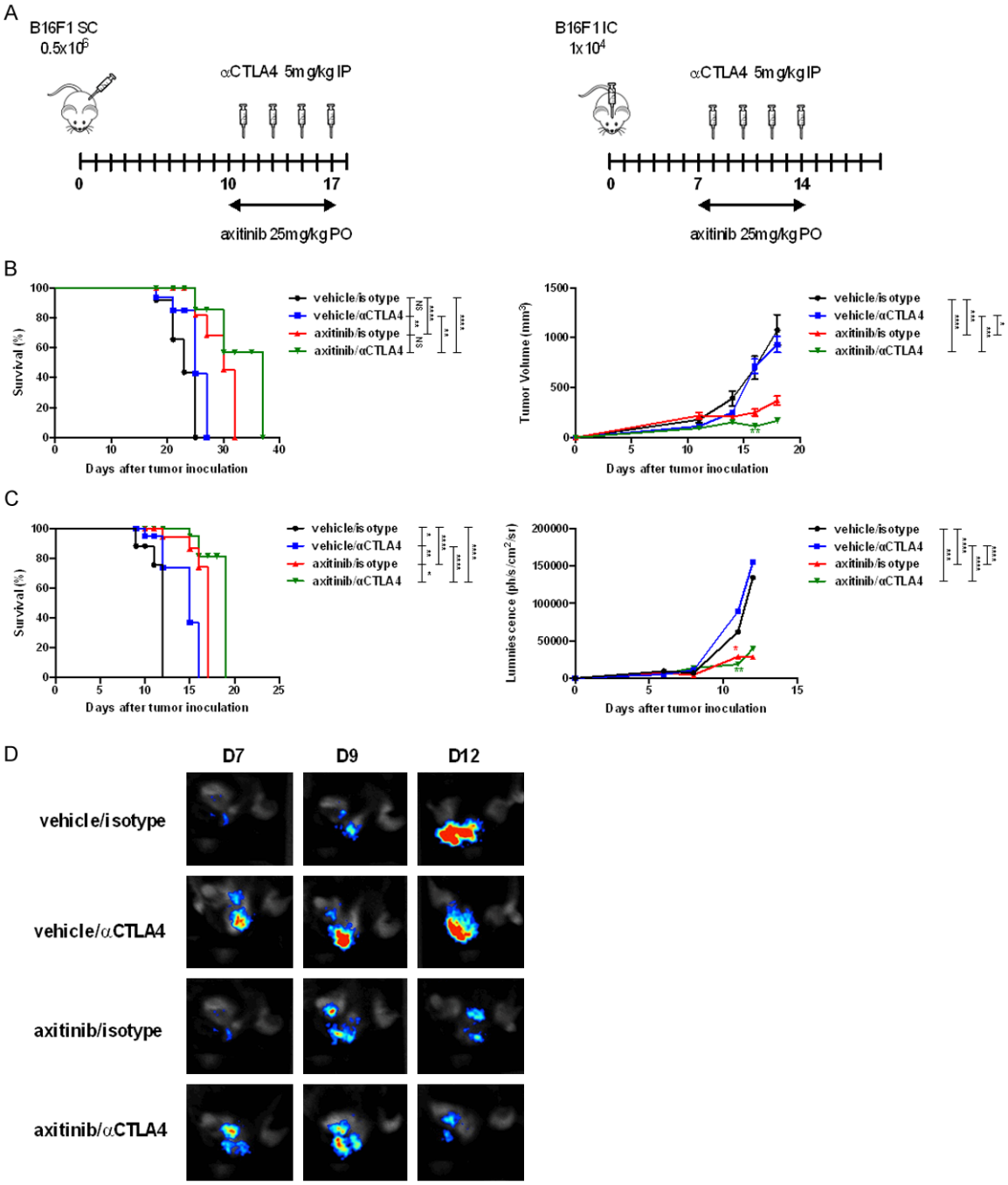

Figure 1. Axitinib+αCTLA4 reduces tumor growth and increases survival in subcutaneous and intracranial mouse models. A. Treatment schedule of subcutanous and intracranial tumor-bearing mice. C57BL/6 mice were subcutaneously or intracranially inoculated with B16F1 cells. For the subcutaneous model, treatment with axitinib was initiated when the tumor was palpable (+/- 150 mm^3) and for the intracranial model, treatment with axitinib was initiated when tumors emited a bioluminescent signal. Vehicle or axitinib was given for a duration of 7 days through oral gavage at a dose of 25 mg/kg, bis in diem (bid). Isotype control or αCTLA4 was given intraperitoneally at a dose of 5 mg/kg on day 2, 4, 6 and 8 after initiation of axitinib treatment. B. Survival curve and mean tumor growth curve of the four treatment groups of the subcutaneous model (n = 2, 5 mice per group); *p < 0.05; **p < 0.01; ***p < 0.001; ****p < 0.0001. C. Survival curve and mean tumor growth curve represented as bioluminescent signal (radiance) of the intracranial model (n = 2, 6 mice per group); *p < 0.05; **p < 0.01; ***p < 0.001; ****p < 0.0001. D. Representative example of bioluminescence imaging of the intracranial tumors according to treatment group. One representative of 2 independent experiments is shown.

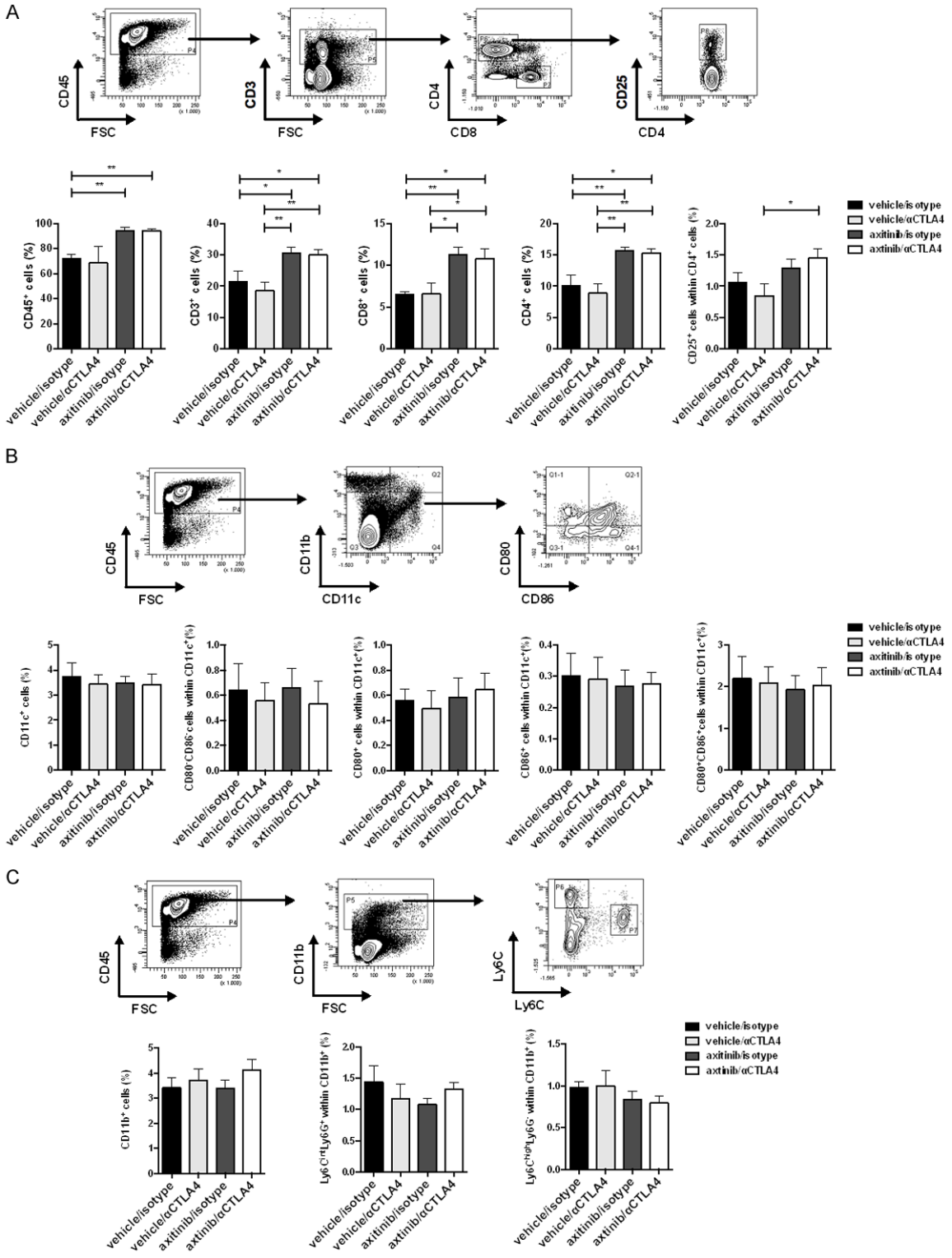

Figure 2. Axitinib+αCTLA4 increases the number of CD4$^+$ and CD8$^+$ T cells in the spleen of subcutaneous tumor-bearing mice. Subcutaneous tumor-bearing mice were treated with vehicle or axitinib for 7 days (25 mg/kg, oral gavage, bid). Isotype control of αCTLA4 was given on day 2, 4 and 6 after initiation of axitinib treatment (intraperitoneal (IP), 5 mg/kg). Mice were sacrificed on the 7th day of axitinib treatment and single cell suspensions of the spleen were made and subsequently analyzed through flow cytometry. A. Gating strategy for determination of the T cells. Percentage of CD45$^+$ cells. Percentage of CD3$^+$ cells within the CD45$^+$ cell population. Percentage of CD8$^+$ and CD4$^+$ cells within the CD3$^+$ cell population. Percentage of CD25$^+$ cells within the CD4$^+$ cell population. B.

Gating strategy for determination of the DCs and their maturation markers. Percentage of $CD11c^+$ cells within the $CD45^+$ cell population. Percentage of respectively the $CD80^-CD86^-$ cells, $CD80^+$ cells, $CD86^+$ and $CD80^+CD86^+$ cells within the $CD11c^+$ cell population. C. Gating strategy for determination of the $CD11b^+$ cells and determination of the MDSCs subsets. Percentage of $CD11b^+$ cells within the $CD45^+$ cell population. Percentage of respectively the $Ly6C^{int}Ly6C^{high}$ cells and $Ly6C^{high}Ly6G^-$ cells within the $CD11b^+$ cell population. Four independent experiments were performed, with 3 mice per group, and results are presented as mean ± SEM; *p < 0.05; **p < 0.01.

Flow cytometry

Data were collected on an LSR Fortessa flow cytometer (BD Biosciences) and analyzed with FACSDiva (BD Biosciences) software.

ELISA

The concentration of interferon-gamma (IFN-γ) (eBioscience), tumor-necrosis factor-alpha (TNF-α) (eBioscience) and interleukin-2 (IL-2) (eBioscience) in culture supernatants was quantified using commercially available ELISA kits according to the manufacturer's instructions. The optical density was measured at 450 nm using a Thermomax microplate reader.

Statistical analysis

Results are presented as mean ± SEM. For the comparison of two groups, Student's t-test (unpaired T-test with equal standard deviation (SD)) was performed. Definition of statistical significance $P < 0.05$. Sample size and number of repetitions for each experiment are indicated in the figure legends. For tumor growth, a two-way ANOVA followed by the Bonferroni multiple comparison test was conducted (significance and confidence level: 0.05 (95% confidence interval)). Sample Survival was visualized in a Kaplan-Meier curve and analyzed by the log-rank (Mantel-Cox) test. All statistical analyses were performed using GraphPad Prism 6.

Results

Axitinib combined with αCTLA-4 reduces tumor growth and increases survival in subcutaneous and intracranial melanoma models

To investigate whether axitinib+αCTLA-4 combination treatment had an enhanced effect on tumor growth and survival compared to the respective monotherapies, we randomized subcutaneous and intracranial B16F1 tumor-bearing mice in four treatment groups: vehicle/isotype, vehicle/αCTLA-4, axitinib/isotype and axitinib/αCTLA-4 (**Figure 1A**). For the purpose of clarity and consistency, hereafter, we will refer to these groups as respectively control, αCTLA, axitinib and combination group.

Axitinib+αCTLA-4 treatment significantly inhibited tumor growth as compared to the control and αCTLA-4 groups in both the subcutaneous (**Figure 1B**) and intracranial (**Figure 1C** and **1D**) models. In addition, in the subcutaneous model there was a trend towards a reduction of tumor growth in the combination group as compared to the axitinib group. In contrast to the αCTLA-4 group, in the axitinib group, tumor growth was also significantly reduced as compared to the control group.

In both models, survival was significantly increased in the axitinib and axitinib+αCTLA-4 groups as compared to the control and αCTLA-4 groups (**Figure 1B** and **1C**). In the intracranial model, we also found a significant survival benefit in the αCTLA-4 group when compared to the control group. Moreover, in the axitinib+αCTLA-4 group there was a significant increased survival as compared to the axitinib group (**Figure 1C**). Median survival in the axitinib+αCTLA-4 group was considerably longer as compared to the axitinib group in the subcutaneous model (resp. 37 days vs. 30 days (**Figure 1B**).

In conclusion, these results suggest that the combination of axitinib with αCTLA-4 leads to a stronger reduction in tumor growth and an increased survival in both subcutaneous and intracranial melanoma mouse models when compared to monotherapy with axitinib or αCTLA-4.

Addition of αCTLA-4 to axitinib treatment does not further increase the number of $CD4^+$ and $CD8^+$ T cells in the spleen of B16F1 subcutaneous tumor-bearing mice

We previously demonstrated that axitinib treatment increases the number of $CD8^+$ T cells in the spleen of mice subcutaneously inoculated with the immunogenic MO4 (B16-OVA) tumor

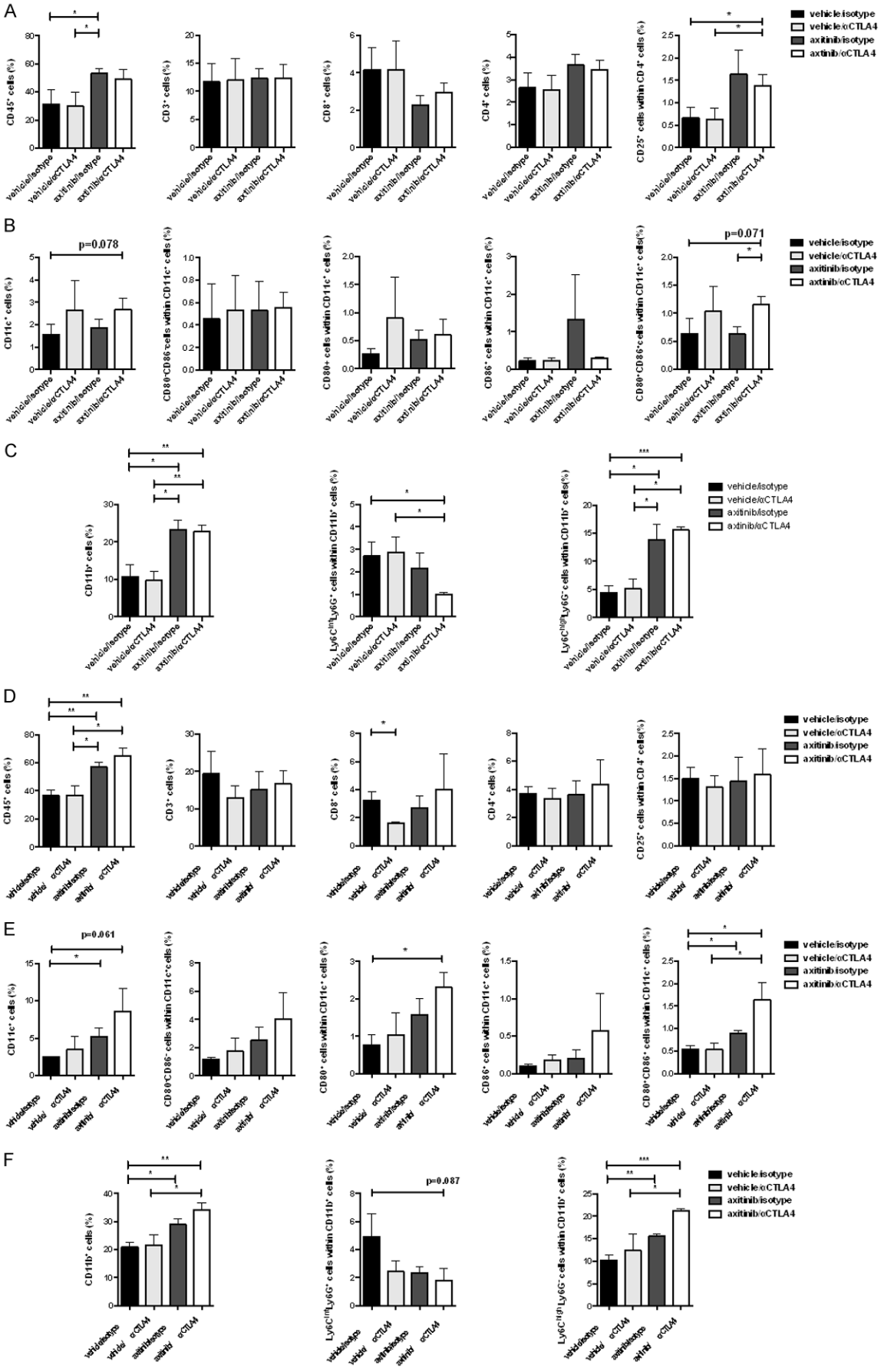
A
B
C
D
E
F
vehicle/isotype
vehicle/αCTLA4
axitinib/isotype
axtinib/αCTLA4
p=0.078
p=0.071
p=0.061
p=0.087

Figure 3. Axitinib+αCTLA4 increases the number of DCs and moMDSCs, but reduces the number of grMDSCs in subcutaneous and intracranial tumors. Subcutaneous and intracranial tumor-bearing mice were treated with vehicle or axitinib for 7 days (25 mg/kg, oral gavage, bid). Isotype control or αCTLA4 was given on day 2, 4 and 6 after initiation of axitinib treatment (IP, 5 mg/kg). Mice were sacrificed on the 7th day of vehicle or axitinib treatment and single cell suspensions of the tumors were made and subsequently analyzed through flow cytometry. A (Subcutaneous tumor) and D (Intracranial tumor) Percentage of $CD45^+$ cells. Percentage of $CD3^+$ cells within the $CD45^+$ cell population. Percentage of $CD8^+$ and $CD4^+$ cells within the $CD3^+$ cell population. Percentage of $CD25^+$ cells within the $CD4^+$ cell population. B (Subcutaneous tumor) and E (Intracranial tumor) Percentage of $CD11c^+$ cells within the $CD45^+$ cell population. Percentage of respectively the $CD80^-CD86^-$ cells, $CD80^+$ cells, $CD86^+$ and $CD80^+CD86^+$ cells within the $CD11c^+$ cell population. C (Subcutaneous tumor) and F (intracranial tumor) Percentage of $CD11b^+$ cells within the $CD45^+$ cell population. Percentage of respectively the $Ly6C^{int}Ly6C^{high}$ cells and $Ly6C^{high}Ly6G^-$ cells within the $CD11b^+$ cell population. Three independent experiments were performed, with 3 mice per group, and results are presented as mean ± SEM; *p < 0.05; **p < 0.01; ***p < 0.001.

cell line [16]. To assess whether combining axitinib with αCTLA-4 could further enhance these effects, we analyzed the spleen of mice subcutaneously inoculated with the poorly immunogenic B16F1 cell line.

In both the axitinib and the axitinib+αCTLA-4 group we found a significantly increased number of $CD45^+$ cells as compared to the control and the αCTLA-4 group. In both groups we also found a significant increased number of $CD3^+$, $CD4^+$ and $CD8^+$ T cells as compared to the control and αCTLA-4 group (**Figure 2A**). However, an increased number of T_{reg} was observed, which reached statistical significance for the axitinib+αCTLA-4 group as compared to the αCTLA-4 group ($p = 0.0232$) (**Figure 2A**). No significant differences were found in the other immune cells populations ($CD11c^+$ cells (DCs), $CD11b^+$ cells, $CD11b^+Ly6C^{high}Ly6G^-$ cells (moMDSCs) or $CD11b^+Ly6C^{int}Ly6G^+$ cells (grMDSCs)) (**Figure 2B** and **2C**).

The addition of αCTLA-4 to axitinib treatment did not further increase the number of $CD4^+$ or $CD8^+$ T cells in the spleen.

αCTLA-4 alone or in combination with axitinib increases the presence of antigen-specific T cells in the spleen

Since we found an increased number of $CD8^+$ T cells in the spleen of tumor-bearing mice treated with axitinib+αCTLA-4, we investigated whether this treatment also affects the number of antigen-specific $CD8^+$ T cells in the spleen. Splenocytes were isolated from subcutaneous tumor-bearing mice and restimulated with Tyrosinase-Related Protein 2 (TRP-2) peptide. Due to its expression in both melanocytes and melanoma, TRP-2 is reported as a melanoma rejection antigen. Proliferation and cytokine secretion of $CD8^+$ T cells were evaluated after 72 h of restimulation. In the αCTLA-4 and axitinib+αCTLA-4 group we observed an increased proliferation accompanied by a significantly increased IFNγ, IL-2 and TNFα production in response to the TRP-2 peptide. This was even more pronounced in the combination group (**Figure 4A**).

These results suggest that αCTLA-4 increases the number of antigen-specific $CD8^+$ T cells in the spleen of tumor-bearing mice. This effect was maintained and enhanced when combined with axitinib treatment.

Axitinib combined with αCTLA-4 reduces the number of granulocytic MDSCs in subcutaneous tumors and increases the number of matured DCs in intracranial tumors

We further investigated the effect of these treatments on the immune cells present in the tumor microenvironment.

In the subcutaneous and intracranial tumors we observed a significant increase in the number of tumor-infiltrating immune cells in the axitinib and axitinib+αCTLA-4 group as compared to the control and αCTLA-4 group (**Figure 3A** and **3D**). We found a significantly increased number of T_{reg} in the axitinib+αCTLA-4 group as compared to the control and αCTLA-4 groups, respectively, in the subcutaneous model, but not in the intracranial model. No s ignificant differences in the $CD4^+$ and $CD8^+$ T cells were found in the different treatment groups (**Figure 3A** and **3D**).

Investigation of the DCs and their maturation markers showed a non-significant trend towards increased number of DCs in the αCTLA-4 and axitinib+αCTLA-4 group as compared to the control and axitinib group in the subcutaneous model. In those groups we also found an increased expression of maturation markers, which was significant in the axitinib+αCTLA-4

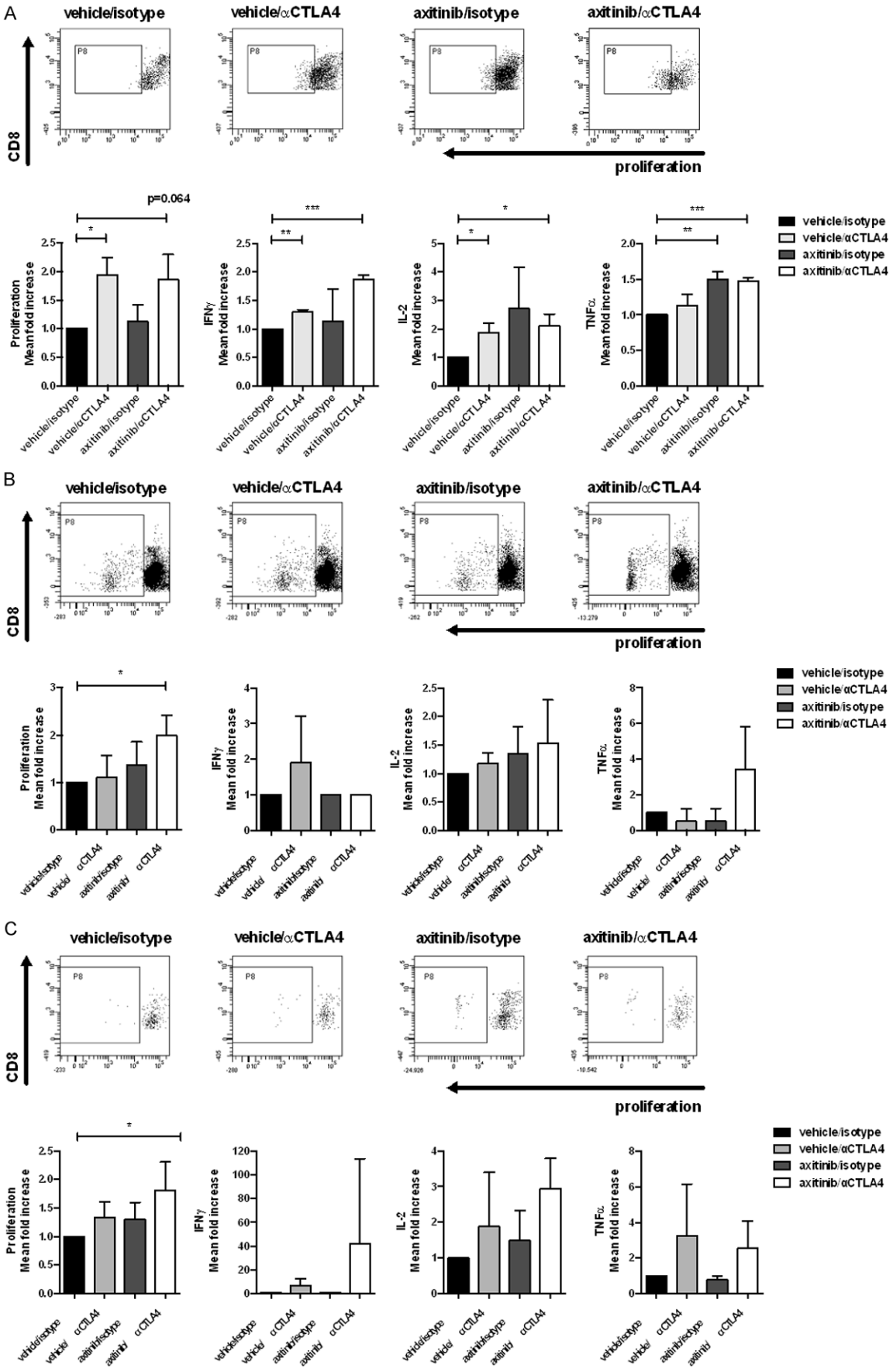
A
vehicle/isotype
vehicle/αCTLA4
axitinib/isotype
axitinib/αCTLA4
CD8
proliferation
P8
p=0.064
Proliferation Mean fold increase
IFNγ Mean fold increase
IL-2 Mean fold increase
TNFα Mean fold increase
B
C

Figure 4. Axitinib+αCTLA4 increases the number of antigen-specific $CD8^+$ T cells within the spleen and increases the antigen-presenting function of intratumoral DCs. A. Subcutaneous tumor-bearing mice were treated with vehicle or axitinib for 7 days (25 mg/kg, oral gavage, bid). Isotype control or αCTLA4 was given on day 2, 4 and 6 after initiation of axitinib treatment (IP, 5mg/kg). Mice were sacrificed on the 7th day of axitinib treatment and single cell suspensions of the spleen were made and $CD8^+$ T cells were restimulated with TRP-2 (5 μM). Proliferation and cytokine production were analyzed after 72 h. Representative FACS profile of the determination of the $CD8^+$ T-cell proliferation. Proliferation of $CD8^+$ T cells after 72 h of restimulation expressed as mean fold increase. IFNγ, IL-2 and TNFα secretion as determined after 72 h of restimulation and expressed as mean fold increase. Controls included T cells cultured in the absence of MDSCs with and without T-cell stimulation. B (subcutaneous tumor) and C. (intracranial tumor) DCs were sorted from subcutaneous or intracranial tumor-bearing mice that were treated with vehicle or axitinib for 7 days (25 mg/kg, oral gavage, bid) and isotype control or αCTLA4 on day 2, 4 and 6 after initiation of axitinib treatment (IP, 5 mg/kg). These intratumoral DCs were co-cultured with $CD8^+$ T cells sorted from the spleen of naïve pmel mice at a 1:10 ratio (DC:$CD8^+$ T cells). Proliferation and cytokine production were analyzed after 72 h. Controls included T cells cultured in the absence of MDSCs with and without T-cell stimulation. Representative FACS profiles of the determination of $CD8^+$ T-cell (pmel) proliferation. Proliferation of the $CD8^+$ T cells after 72 h of co-culture expressed as mean fold increase. IFNγ, IL-2 and TNFα secretion as determined after 72 h of co-culture and expressed as mean fold increase. Three (or two for subcutaneous DCs) independent experiments were performed with 3 mice per group, spleens or tumors were pooled per group before cell sorting, and results are presented as mean ± SEM; *$p < 0.05$; **$p < 0.01$; ***$p < 0.001$.

when compared to the axitinib group (**Figure 3B**). In the intracranial model, we observed a significant increased number of DCs and expression of maturation markers in the axitinib and axitinib+αCTLA-4 groups. However, this increase was more pronounced in the combination group (**Figure 3E**).

Investigation of the $CD11b^+$ cells, moMDSCs ($CD11b^+Ly6C^{high}Ly6G^-$ cells) and grMDSCs ($CD11b^+Ly6C^{int}Ly6G^+$ cells) showed a significantly increased number of $CD11b^+$ cells in the axitinib and axitinib+αCTLA group as compared to the control and αCTLA groups in the subcutaneous model and intracranial model. Moreover, in both tumor models we found a significantly increased number of moMDSCs in the axitinib and axitinib+αCTLA-4 group as compared to the control and αCTLA-4 group. Additionally, in the subcutaneous model we observed a significant reduction of the number of grMDSCs in the axitinib+αCTLA-4 group as compared to the control group. In contrast, in the intracranial model, no significant reduction in the number of grMDSCs was observed in the treatment groups as compared to the control group (**Figure 3C** and **3F**).

Overall, axitinib increases the number of tumor-infiltrating immune cells, more specifically $CD11b^+$ cells and moMDSCs. This effect was maintained in the combination treatment. αCTLA-4 increased the number of mature DCs in the subcutaneous model. The additional benefit of the combination treatment was translated in a significant reduction of the number of grMDSCs in the subcutaneous tumors and a significantly increased number of mature DCs in the intracranial tumor.

Axitinib combined with αCTLA-4 increases the antigen-presenting capacity of intratumoral DCs

Since we observed an increased number of mature DCs in the subcutaneous and intracranial tumors, respectively in the αCTLA-4 and axitinib+αCTLA-4 group, we investigated whether the antigen-presenting function of these DCs was affected by the treatment. Therefore we sorted DCs from subcutaneous and intracranial tumors and co-cultured them with $CD8^+$ T cells isolated from naïve pmel transgenic mice. Proliferation and cytokine secretion was analyzed after 72 h. In both subcutaneous and intracranial models, we found a significantly increased proliferation of $CD8^+$ T cells in the axitinib+αCTLA-4 group as compared to the control group. This effect was not observed in the axitinib and αCTLA-4 group. This was accompanied by an increased production of IL-2 and TNFα in the axitinib+αCTLA-4 group (**Figure 4B** and **4C**).

These results suggest that the combination of axitinib with αCTLA-4 increases the antigen-presenting capacity of intratumoral DCs.

Axitinib, αCTLA-4 and axitinib combined with αCTLA-4 lead to a reduced suppressive capacity of intratumoral moMDSCs

Since we have shown that addition of αCTLA-4 to axitinib treatment further increased the

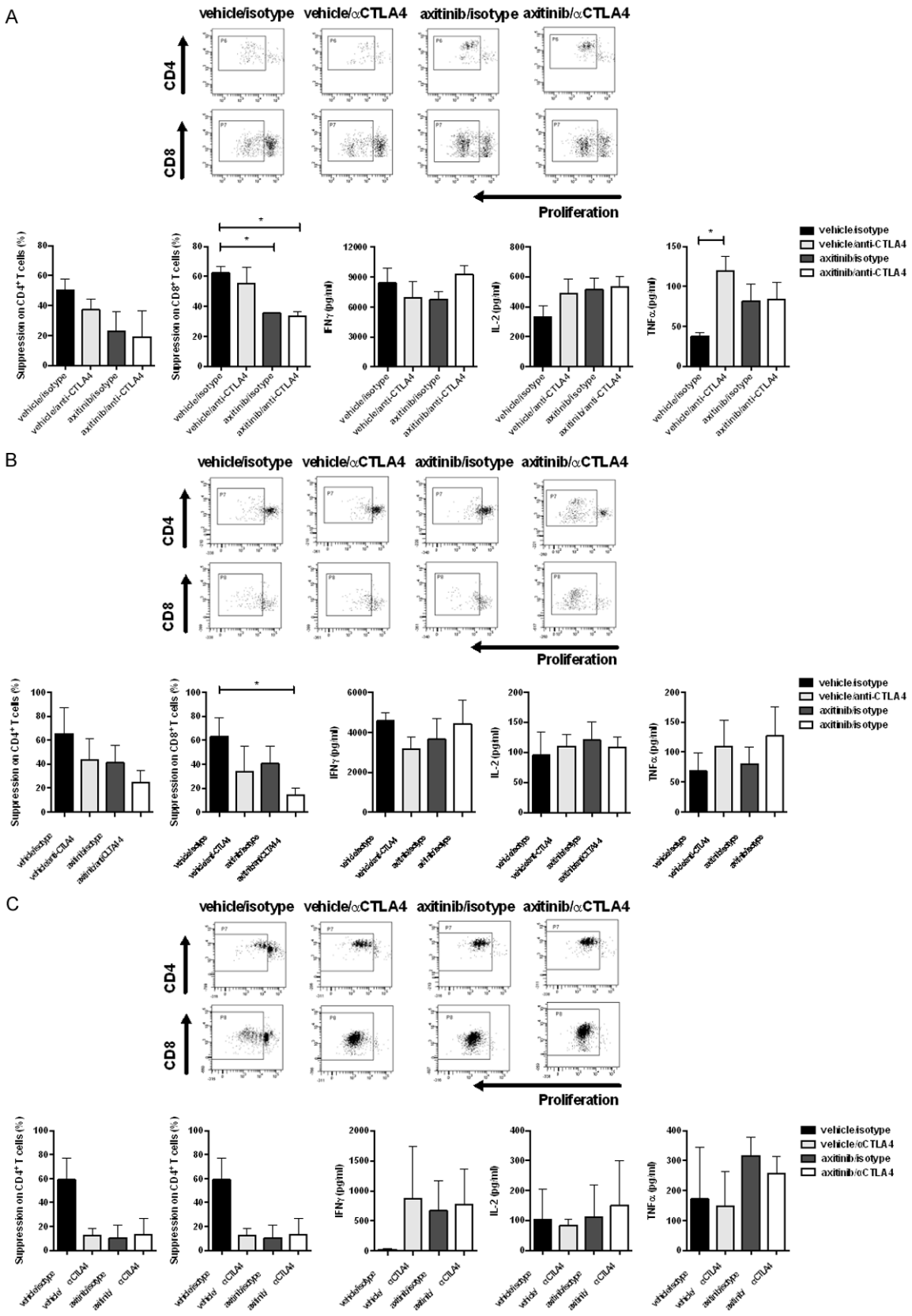

Figure 5. Axitinib+αCTLA4 reduces the suppressive capacity of moMDSCs sorted from the spleens of subcutaneous tumor-bearing mice and from the subcutaneous and intracranial tumors. Monocytic MDSCs were sorted from either the spleens of subcutaneous tumor-bearing mice or from the subcutaneous or intracranial tumors of mice

treated with vehicle or axitinib for 7 days (25 mg/kg, oral gavage, bid) and isotype control or αCTLA4 on day 2, 4 and 6 after initiation of axitinib treatment (IP, 5 mg/kg). These moMDSCs were co-cultured with splenocytes isolated from the spleen of naïve C57BL/6 mice at different moMDSC:T cell ratios in the presence of anti-CD3/CD28 beads. Proliferation and cytokine production were analyzed after 72 h. Controls included T cells cultured in the absence of MDSCs with and without T-cell stimulation. A. moMDSCs sorted from the spleen of tumor-bearing mice. Representative FACS profiles of the determination of the $CD4^+$ and $CD8^+$ T cell proliferation in a 1:8 (moMDSC:T cell) ratio. Percentage of suppression of moMDSCs on $CD4^+$ and $CD8^+$ T cells at a 1:8 ratio after 72 h of co-culture. IFNγ, IL-2 and TNFα secretion as determined after 72 h of co-culture. B. Intratumoral moMDSCs in the subcutaneous model. Representative FACS profiles of the determination of the $CD4^+$ and $CD8^+$ T cell proliferation in a 1:10 (moMDSC:T cell) ratio. Percentage of suppression of moMDSCs on $CD4^+$ and $CD8^+$ T cells at a 1:10 ratio after 72 h of co-culture. IFNγ, IL-2 and TNFα secretion as determined after 72 h of co-culture. C. Intratumoral moMDSCs in the intracranial model. Representative FACS profiles of the determination of the $CD4^+$ and $CD8^+$ T cell proliferation in a 1:4 (moMDSC:T cell) ratio. Percentage of suppression of moMDSCs on $CD4^+$ and $CD8^+$ T cells at a 1:4 ratio after 72 h of co-culture. IFNγ, IL-2 and TNFα secretion as determined after 72 h of co-culture. Two independent experiments were performed with 3 mice per group, spleens or tumors were pooled per group before cell sorting, and results are presented as mean ± SEM; *$p < 0.05$.

number of moMDSCs and since we previously showed that axitinib reduces the suppressive capacity of moMDSCs, we investigated whether axitinib+αCTLA-4 affected the suppressive function of moMDSCs. Therefore we sorted moMDSCs from the spleens of subcutaneous tumor-bearing mice and from the intracranial and subcutaneous tumors. We co-cultured these moMDSCs with stimulated splenocytes derived from naïve mice in a 1:8 (spleen), 1:10 (subcutaneous) and 1:4 (intracranial) ratio (moMDSC:T cell). After 72 h, proliferation and cytokine secretion were analyzed.

In the spleen we observed a significant reduction of the suppressive capacity of moMDSCs on $CD8^+$ T cells in both the axitinib and axitinib+αCTLA-4 group. In the subcutaneous tumors we found a reduction of the suppressive capacity of these moMDSCs on $CD8^+$ T cells in both the αCTLA-4 and axitinib group, but these were not statistically significant. However, when both treatments were combined, a stronger and significant reduction of the suppressive function was obtained. In both the spleen and the subcutaneous tumor, the reduction of the suppressive capacity was less pronounced on $CD4^+$ T cells in the axitinib and αCTLA-4, but the suppressive function on $CD4^+$ T cells is strongly reduced in the combination group. In the intracranial model, we found a strong reduction of the suppressive capacity of intratumoral moMDSCs in all treatment groups (**Figure 5A-C**).

When cytokine secretion was analyzed no significant changes were observed in all treatment groups (**Figure 5A-C**).

These results suggest that the combination of axitinib with αCTLA-4 reduces the suppressive capacity of moMDSCs sorted from the spleen, subcutaneous and intracranial tumors.

Axitinib, αCTLA-4 and axitinib combined with αCTLA-4 induce an antigen-presenting function in intratumoral monocytic MDSCs present in the subcutaneous tumor, but not in the intracranial tumors

Previously we have shown that axitinib induces an antigen-presenting function in moMDSCs sorted from MO4 subcutaneous tumors, but not from intracranial tumors [20]. Since we showed that the combination of axitinib with αCTLA-4 further reduces the suppressive capacity of intratumoral moMDSCs in the subcutaneous model, we investigated whether there was also an increased antigen-presenting capacity of these moMDSCs after axitinib+αCTLA-4 treatment. Therefore moMDSCs sorted from subcutaneous or intracranial tumors were co-cultured with $CD8^+$ T cells isolated from naïve C3H mice at different ratios.

In the subcutaneous model, we observed an increase in $CD8^+$ T-cell proliferation (**Figure 6A**) and cytokine secretion (IFNγ, IL-2 and TNFα) (**Figure 6B**) in the three treatment groups as compared to the control group. At a 1:10 ratio, we did not observe an additional effect of combining both treatments. However, at a 1:20 and 1:40 ratio we observed a more pronounced increase in the proliferation and cytokine secretion in the combination group.

However, in the intracranial tumor model we did not find specific differences between the different treatment groups (data not shown).

These results suggest that treatment with αCTLA-4, axitinib and especially with the com-

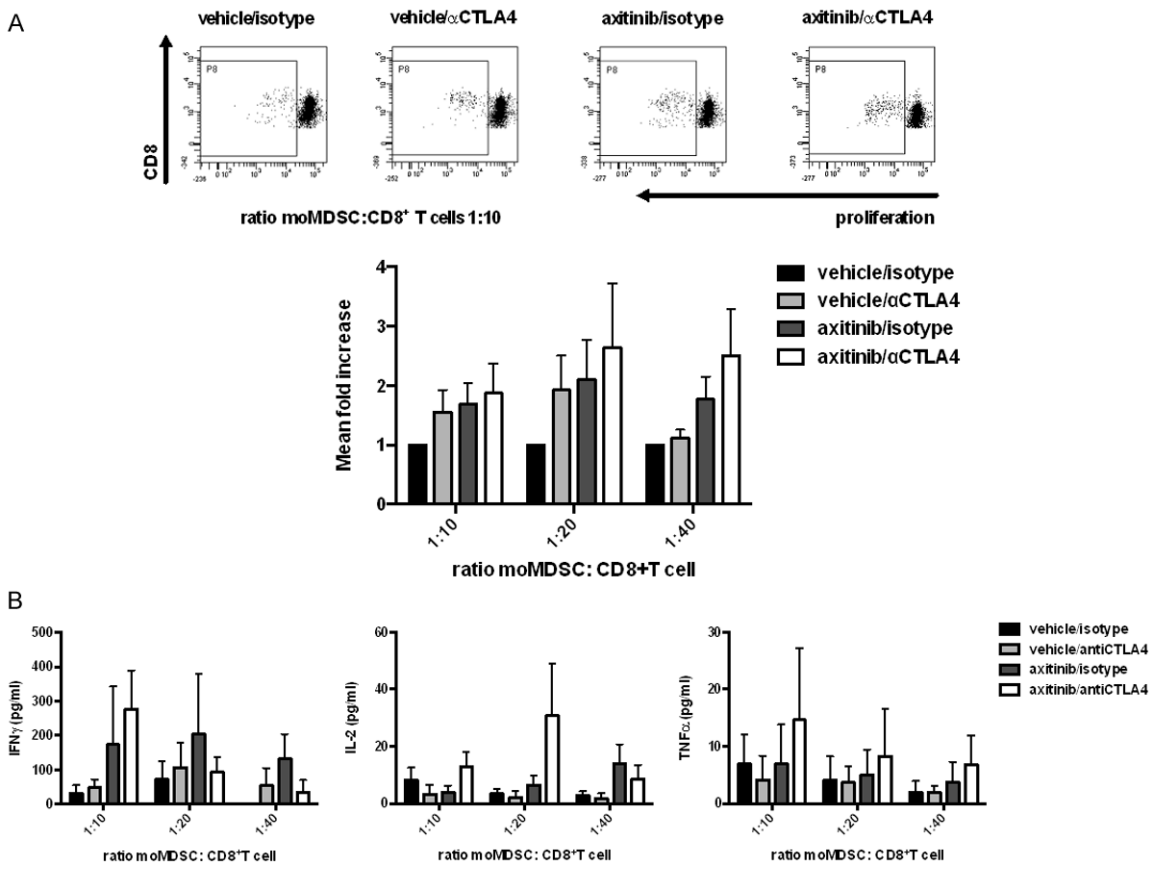

Figure 6. Axitinib+αCTLA4 induces an antigen-presenting function in subcutaneous intratumoral moMDSCs. Monocytic MDSCs were sorted from either the spleens of subcutaneous tumor-bearing mice or from the subcutaneous or intracranial tumors of mice treated with vehicle or axitinib for 7 days (25 mg/kg, oral gavage, bid) and isotype control or αCTLA4 on day 2, 4 and 6 after initiation of axitinib treatment (IP, 5 mg/kg). These moMDSCs were co-cultured with $CD8^+$ T cells sorted from the spleen of naïve C3H mice at a 1:10, 1:20 and 1:40 (moMDSC:$CD8^+$ T cell) ratio. Proliferation and cytokine production were analyzed after 72 h. Controls included $CD8^+$ T cells cultured in the absence of MDSCs with and without T-cell stimulation. A. Representative FACS profiles of the determination of the $CD8^+$ T cell proliferation in a 1:10 (moMDSC:$CD8^+$ T cell) ratio. Proliferation of $CD8^+$ T cells (C3H) after 72 h of co-culture expressed as mean fold increase. B. IFNγ, IL-2 and TNFα secretion as determined after 72 h of co-culture. Three independent experiments were performed with 3 mice per group, spleens or tumors were pooled per group before cell sorting, and results are presented as mean ± SEM; *$p < 0.05$.

bination of axitinib+αCTLA-4 induces an antigen-presenting capacity in moMDSCs sorted from subcutaneous tumors, but not from intracranial tumors.

Discussion

In this study we show that the combination of axitinib with αCTLA-4 significantly increased survival in intracranial and subcutaneous melanoma mouse models. Moreover, we also demonstrate that axitinib combined with αCTLA-4 increases the antigen-presenting capacity of intratumoral DCs, reduces the number of grMDSCs and increases the number of moMDSCs with a reduced suppressive capacity in subcutaneous and intracranial tumors. However, an antigen-presenting capacity after axitinib+αCTLA-4 treatment was only induced in the moMDSCs isolated from subcutaneous tumors. Together these results demonstrate that the combination of VEGFR-blockade with CTLA-4-blockade enhances the antigen-specific antitumor immune response and skews the immunosuppressive tumor microenvironment towards an immune stimulating one.

To our knowledge this is the first time that the effect of the combination of VEGFR-blockade with CTLA-4-blockade on immune cells is extensively examined in subcutaneous and intracranial melanoma mouse models. Similar to

our previous results obtained with axitinib in a more immunogenic MO4 (B16-OVA) model, we found that axitinib increased the number of $CD4^+$ and $CD8^+$ T cells in the spleen of subcutaneous tumor-bearing mice. The addition of αCTLA-4 treatment did not further increase the frequencies of T cells, but increased the number of antigen-specific $CD8^+$ T cells in the spleen. These results are in line with previous findings, which show that CTLA-4 blockade induces an immune memory in preclinical models and increases the antigen-specific $CD8^+$ T cell numbers in prevaccinated patients with melanoma [23, 24].

Several changes in the immune cell populations were found in the tumor microenvironment in the different treatment groups. Firstly, in the spleen and in the subcutaneous tumor we found a significantly increased number of T_{reg} in the combination group. Since the markers we used to define T_{reg} are shared with activated T cells, we sorted them from the spleen of these tumor–bearing mice. We did not find a significant reduction in the suppressive capacity of T_{reg} in the several treatment groups (data not shown). Several studies demonstrated that αCTLA-4 treatment expands T_{reg} in lymphoid organs and blood of both mice and humans [25, 26]. In contrast, when CTLA-4 blockade was combined with a vaccine consisting of irradiated tumor cells transduced to express GM-CSF (Gvax) an increased ratio of effector T cells to T_{reg} was present in the tumor. The fact that we did not find this increased ratio in our treatment model is probably due to the absence of antigen-specific vaccination.

Secondly, CTLA-4 blockade in monotherapy and in combination with axitinib increased the number of mature DCs. When these were sorted from intracranial and subcutaneous tumors we observed a significantly increased antigen-presenting capacity in the combination group, but not in the αCTLA-4 or axitinib group. VEGF is known to inhibit the maturation of DCs and monoclonal antibodies against VEGF increased the endogenous DC function [12, 27]. In this study we mainly found a significantly increased antigen-presenting capacity when VEGFR-blockade was combined with CTLA-4 blockade. It has been shown that CTLA-4 reduced the expression of CD80 and CD86 on DCs through transendocytosis [28]. In this study we also demonstrate that CTLA-4 blockade increases the expression of CD80 and CD86 on intratumoral DCs. Furthermore, it has been shown that CTLA-4 is expressed by human DCs and influences their maturation and antigen presentation [29]. Combining VEGFR- and CTLA-4 blockade probably increases the DC maturation and their antigen-presenting capacity through reduction of these suppressive mechanisms.

Thirdly, a reduced number of grMDSCs was found in the subcutaneous tumors in the combination arm. In the intracranial tumors, this reduction was seen in all treatment groups. In melanoma patients it was shown that ipilimumab reduces the number and suppressive capacity of circulating grMDSCs [18]. However, in renal cell carcinoma patients treatment with bevacizumab did not decrease the number of MDSCs [30]. So, the effect of axitinib on these grMDSCs is probably indirect. In our study, we tried to investigate the suppressive capacity of these intratumoral grMDSCs, however we did not obtain a sufficient number of cells to perform functional assays (data not shown). In contrast to the grMDSCs, we observed an increased number of moMDSCs in the axitinib and axitinib+αCTLA-4 group. These results are consistent with our previous data obtained with axitinib in an immunogenic MO4 model.

Moreover, when these moMDSCs were sorted from the spleen, the subcutaneous or intracranial tumor, we found that they had a reduced suppressive capacity. Since there was no additional effect of the combination therapy in the spleen, this reduced suppressive capacity can be attributed to the effect of axitinib. In the subcutaneous and intracranial tumors, there was a reduction of the suppressive capacity in both the monotherapy groups and the combination group. We only found an additional reduction in the combination group in the subcutaneous tumor. In addition, in the subcutaneous tumor, these cells acquired an antigen-presenting function. To our knowledge this is the first time that the effect of CTLA-4 blockade with or without VEGFR-blockade on the function of moMDSCs has been studied. In melanoma patients, treatment with ipilimumab reduced the number of circulating moMDSC and a greater decrease was associated with an improved progression-free survival (PFS) [19]. In the subcutaneous model, we demonstrate that the moMDSCs acquired an antigen-presenting function in the

three treatment groups. However, this was not the case for the intracranial model. These results are consistent with our previous findings obtained with axitinib in the MO4 melanoma model. The fact that the moMDSCs sorted from intracranial tumors did not obtain an antigen-presenting function is probably related to the naturally immunosuppressive microenvironment of the central nervous system (anatomically protected by blood brain barrier, paucity of professional antigen presenting cells, low levels of Major Histocompatibility Complex (MHC) molecule expression and constitutive expression of immunosuppressive cytokines, such as IL-10 and TGF-β). In an ovarian carcinoma mouse model, it was shown that CTLA-4 is upregulated on the surface of MDSCs isolated out of the spleen of tumor-bearing mice and that CTLA-4 blockade reduces their arginase I production [31]. Despite the fact that the authors did not differentiate between granulocytic and monocytic MDSCs, this reduced arginase I production could be a possible mechanism for reduced suppressive function of moMDSCs in the intracranial model.

In conclusion, our results suggest that the supportive effect on tumor growth and survival of VEGFR- and CTLA-4 blockade is in part due to an enhanced antitumor immune response generated by an increased number of antigen-specific $CD8^+$ T cells in the spleen and an increased antigen-presenting function of intratumoral DCs in combination with a reduction of the immunosuppressive tumor microenvironment, mainly the suppressive MDSCs. Although the combination treatment did not always lead to a significantly increased effect as compared to each treatment alone, our results suggest that an increased antitumor immune response can be obtained through combination of antiangiogenesis and immunotherapy. Currently multiple combinations with different immunotherapies are being investigated and further investigations are necessary to find the optimal combination treatment, especially in the treatment of melanoma brain metastases.

Acknowledgements

The authors thank Angelo Willems for expert assistance with the cell sorting. Sarah K Maenhout and Stephanie Du Four are funded by a PhD grant from the Agency for Innovation by Science and Technology in Flanders (IWT). This work is supported by a grant from the Research Foundation Flanders (Fonds voor Wetenschappelijk Onderzoek (FWO, G02341-1N)) to Kris Thielemans and Joeri L Aerts. The FACS AriaIII cell sorter and the LSR Fortessa were purchased with support from the Hercules Foundation to Kris Thielemans and Joeri L Aerts (grant UABR/09/002) and the Foundation against Cancer (Stichting Tegen Kanker), respectively.

Disclosure of conflict of interest

None.

Address correspondence to: Joeri L Aerts, Laboratory of Molecular and Cellular Therapy, Vrije Universiteit Brussel, Laarbeeklaan 103E, 1090 Jette, Belgium. Tel: +32-2 477 45 69; Fax: +32-2 477 45 68; E-mail: Joeri.Aerts@vub.ac.be

References

[1] Bafaloukos D and Gogas H. The treatment of brain metastases in melanoma patients. Cancer Treat Rev 2004; 30: 515-520.

[2] Chapman PB, Hauschild A, Robert C, Haanen J, Ascierto PA, Larkin J, Dummer R, Garbe C, Testori A, Maio M, Hogg D, Lorigan P, Lebbe C, Jouary T, Schadendorf D, Ribas A, O'Day SJ, Sosman J, Kirkpatrick JP, Eggermont A, Dreno B, Nolop K, Nelson B, Hou J, Lee RJ, Flaherty KT and McArthur GA. Improved Survival with Vemurafenib in Melanoma with BRAF V600E Mutation. N Engl J Med 364: 2507-2516.

[3] Hauschild A, Grob JJ, Demidov LV, Jouary T, Gutzmer R, Millward M, Rutkowski P, Blank CU, Miller WH, Kaempgen E, Martín-Algarra S, Karaszewska B, Mauch C, Chiarion-Sileni V, Martin AM, Swann S, Haney P, Mirakhur B, Guckert ME, Goodman V and Chapman PB. Dabrafenib in BRAF-mutated metastatic melanoma: a multicentre, open-label, phase 3 randomised controlled trial. The Lancet 2012; 380: 358-365.

[4] Flaherty KT, Robert C, Hersey P, Nathan P, Garbe C, Milhem M, Demidov LV, Hassel JC, Rutkowski P, Mohr P, Dummer R, Trefzer U, Larkin JM, Utikal J, Dreno B, Nyakas M, Middleton MR, Becker JC, Casey M, Sherman LJ, Wu FS, Ouellet D, Martin AM, Patel K, Schadendorf D and Group MS. Improved survival with MEK inhibition in BRAF-mutated melanoma. N Engl J Med 2012; 367: 107-114.

[5] Hodi FS, O'Day SJ, McDermott D, Weber RW, Sosman JA, Haanen J, Gonzalez R, Robert C, Schadendorf D, Hassel JC, Akerley W, van den Eertwegh AJ, Lutzky J, Lorigan P, Vaubel JM,

Linette GP, Hogg D, Ottensmeier CH, Lebbe C, Peschel C, Quirt I, Clark JI, Wolchock JD, Weber J, Tian J, Yellin MJ, Nichol GM, Hoos A and Urba WJ. Improved Survival with Ipilimumab in Patients with Metastatic Melanoma. N Engl J Med 2010; 363: 711-723.

[6] Robert C, Long GV, Brady B, Dutriaux C, Maio M, Mortier L, Hassel JC, Rutkowski P, McNeil C, Kalinka-Warzocha E, Savage KJ, Hernberg MM, Lebbe C, Charles J, Mihalcioiu C, Chiarion-Sileni V, Mauch C, Cognetti F, Arance A, Schmidt H, Schadendorf D, Gogas H, Lundgren-Eriksson L, Horak C, Sharkey B, Waxman IM, Atkinson V and Ascierto PA. Nivolumab in previously untreated melanoma without BRAF mutation. N Engl J Med 2015; 372: 320-330.

[7] Robert C, Thomas L, Bondarenko I, O'Day SJ, Weber J, Garbe C, Lebbe C, Baurain JF, Testori A, Grob JJ, Davidson N, Richards J, Maio M, Hauschild A, Miller WH, Gascon P, Lotem M, Harmankaya K, Ibrahim R, Francis S, Chen TT, Humphrey R, Hoos A and Wolchock JD. Ipilimumab plus Dacarbazine for Previously Untreated Metastatic Melanoma. N Engl J Med 364: 2617-2626.

[8] Long GV, Trefzer U, Davies MA, Kefford RF, Ascierto PA, Chapman PB, Puzanov I, Hauschild A, Robert C, Algazi A, Mortier L, Tawbi H, Wilhelm T, Zimmer L, Switzky J, Swann S, Martin A-M, Guckert M, Goodman V, Streit M, Kirkwood JM and Schadendorf D. Dabrafenib in patients with Val600Glu or Val600Lys BRAF-mutant melanoma metastatic to the brain (BREAK-MB): a multicentre, open-label, phase 2 trial. Lancet Oncol 2012; 13: 1087-1095.

[9] Dummer R, Goldinger SM, Turtschi CP, Eggmann NB, Michielin O, Mitchell L, Veronese L, Hilfiker PR, Felderer L and Rinderknecht JD. Vemurafenib in patients with BRAF(V600) mutation-positive melanoma with symptomatic brain metastases: final results of an open-label pilot study. Eur J Cancer 2014; 50: 611-621.

[10] Margolin K, Ernstoff MS, Hamid O, Lawrence D, McDermott D, Puzanov I, Wolchok JD, Clark JI, Sznol M, Logan TF, Richards J, Michener T, Balogh A, Heller KN and Hodi FS. Ipilimumab in patients with melanoma and brain metastases: an open-label, phase 2 trial. Lancet Oncol 2012; 13: 459-465.

[11] Huang Y, Yuan J, Righi E, Kamoun WS, Ancukiewicz M, Nezivar J, Stantosuosso M, Martin JD, Martin MR, Vianello F, Leblanc P, Munn LL, Huang PH, Duda DG, Fukumura D, Jain RK and Poznansky MC. Vascular normalizing doses of antiangiogenic treatment reprogram the immunosuppressive tumor microenvironment and enhance immunotherapy. Proc Natl Acad Sci U S A 2012; 109: 17561-17566.

[12] Gabrilovich D, Ishida T, Oyama T, Ran S, Kravtsov V, Nadaf S and Carbone DP. Vascular Endothelial Growth Factor Inhibits the Development of Dendritic Cells and Dramatically Affects the Differentiation of Multiple Hematopoietic Lineages In Vivo. Blood 1998; 92: 4150-4166.

[13] Gabrilovich DI, Ostrand-Rosenberg S and Bronte V. Coordinated regulation of myeloid cells by tumours. Nat Rev Immunol 2012; 12: 253-268.

[14] Jain RK. Antiangiogenesis Strategies Revisited: From Starving Tumors to Alleviating Hypoxia. Cancer Cell 2014; 26: 605-622.

[15] Shrimali RK, Yu Z, Theoret MR, Chinnasamy D, Restifo NP and Rosenberg SA. Antiangiogenic agents can increase lymphocyte infiltration into tumor and enhance the effectiveness of adoptive immunotherapy of cancer. Cancer Res 2010; 70: 6171-6180.

[16] Du Four S, Maenhout SK, Depierre K, Renmans D, Niclou SP, Thielemans K, Neyns B and Aerts JL. Axitinib increases the infiltration of immune cells and reduces the suppressive capacity of monocytic MDSCs in an intracranial mouse melanoma model. Oncoimmunology 2015; 4: e998107.

[17] Meyer C, Cagnon L, Costa-Nunes CM, Baumgaertner P, Montandon N, Leyvraz L, Michielin O, Romano E and Speiser DE. Frequencies of circulating MDSC correlate with clinical outcome of melanoma patients treated with ipilimumab. Cancer Immunol Immunother 2014; 63: 247-257.

[18] Pico de Coana Y, Poschke I, Gentilcore G, Mao Y, Nystrom M, Hansson J, Masucci GV and Kiessling R. Ipilimumab treatment results in an early decrease in the frequency of circulating granulocytic myeloid-derived suppressor cells as well as their Arginase1 production. Cancer Immunol Res 2013; 1: 158-162.

[19] Tarhini AA, Edington H, Butterfield LH, Lin Y, Shuai Y, Tawbi H, Sander C, Yin Y, Holtzman M, Johnson J, Rao UN and Kirkwood JM. Immune monitoring of the circulation and the tumor microenvironment in patients with regionally advanced melanoma receiving neoadjuvant ipilimumab. PLoS One 2014; 9: e87705.

[20] Goyvaerts C, De Groeve K, Dingemans J, Van Lint S, Robays L, Heirman C, Reiser J, Zhang XY, Thielemans K, De Baetselier P, Raes G and Breckpot K. Development of the Nanobody display technology to target lentiviral vectors to antigen-presenting cells. Gene Ther 2012; 19: 1133-1140.

[21] Keyaerts M, Remory I, Caveliers V, Breckpot K, Bos TJ, Poelaert J, Bossuyt A and Lahoutte T. Inhibition of firefly luciferase by general anesthetics: effect on in vitro and in vivo bioluminescence imaging. PLoS One 2012; 7: e30061.

[22] Maenhout SK, Van Lint S, Emeagi PU, Thielemans K and Aerts JL. Enhanced suppressive capacity of tumor-infiltrating myeloid-derived suppressor cells compared with their peripheral counterparts. Int J Cancer 2014; 134: 1077-1090.

[23] Leach D, Krummel MF and Allison JP. Enhancement of antitumor immunity by CTLA-4 blockade. Science 1996; 271: 1734-1736.

[24] Yuan J, Ginsberg B, Page D, Li Y, Rasalan T, Gallardo HF, Xu Y, Adams S, Bhardwaj N, Busam K, Old LJ, Allison JP, Jungbluth A and Wolchok JD. CTLA-4 blockade increases antigen-specific CD8(+) T cells in prevaccinated patients with melanoma: three cases. Cancer Immunol Immunother 2011; 60: 1137-1146.

[25] Quezada SA, Peggs KS, Curran MA and Allison JP. CTLA4 blockade and GM-CSF combination immunotherapy alters the intratumor balance of effector and regulatory T cells. J Clin Invest 2006; 116: 1935-1945.

[26] Kavanagh B, O'Brien S, Lee D, Hou Y, Weinberg V, Rini B, Allison JP, Small E and Fong L. CTLA4 blockade expands FoxP3+ regulatory and activated effector CD4+ T cells in a dose-dependent fashion. Blood 2008; 112: 1175-1183.

[27] Gabrilovich D, Ishida T, Nadaf S, Ohm JE and Carbone DP. Antibodies to Vascular Endothelial Growth Factor Enhance the Efficacy of Cancer Immunotherapy by Improving Endogenous Dendritic Cell Function. Clin Cancer Res 1999; 5: 2963-2970.

[28] Qureshi OS, Zheng Y, Nakamura K, Attridge K, Manzotti C, Schimdt EM, Baker J, Jeffery LE, Kaur S, Briggs Z, Hou TZ, Futter CE, Anderson G, Walker LSK and Sansom DM. Trans-endocytosis of CD80 and CD86: A Molecular Basis for the Cell-Extrinsic Function of CTLA-4. Science 2011; 332: 600-603.

[29] Wang XB, Fan ZZ, Anton D, Vollenhoven AV, Ni ZH, Chen XF and Lefvert AK. CTLA4 is expressed on mature dendritic cells derived from human monocytes and influences their maturation and antigen presentation. BMC Immunol 2011; 12: 21.

[30] Rodriguez PC, Ernstoff MS, Hernandez C, Atkins M, Zabaleta J, Sierra R and Ochoa AC. Arginase I-producing myeloid-derived suppressor cells in renal cell carcinoma are a subpopulation of activated granulocytes. Cancer Res 2009; 69: 1553-1560.

[31] Liu Y, Yu Y, Yang S, Zeng B, Zhang Z, Jiao G, Zhang Y, Cai L and Yang R. Regulation of arginase I activity and expression by both PD-1 and CTLA-4 on the myeloid-derived suppressor cells. Cancer Immunol Immunother 2009; 58: 687-697.